

and subtropical amplification of a decadal mode of ENSO from the tropics to the subtropics. However, as discussed in (12), different spatial patterns of midlatitude atmospheric circulating anomalies for ENSO-band and decadal variability suggest that different tropical forcing mechanisms are involved on these two time scales. Thus, the specific mechanism for generating subtropical decadal SST variability in the Pacific gyres appears to be complex and may involve tropical-subtropical ocean-atmosphere interactions other than ENSO.

References and Notes

1. K. E. Trenberth, *Bull. Am. Meteorol. Soc.* **71**, 988 (1990).
2. M. Latif, T. P. Barnett, *Science* **266**, 634 (1994).
3. Y. Zhang, J. M. Wallace, D. S. Battisti, *J. Clim.* **10**, 1004 (1997).
4. C. Deser, M. A. Alexander, M. S. Timlin, *J. Clim.* **9**, 1840 (1996).
5. S. Minobe, *Res. Lett.* **24**, 638 (1997).
6. N. J. Mantua, S. R. Hare, Y. Zhang, J. M. Wallace, R. C. Francis, *Bull. Am. Meteorol. Soc.* **78**, 1069 (1997).
7. A. Gershunov, T. P. Barnett, D. R. Cayan, *Eos Trans. AGU* **80**, 25 (1999).
8. W. B. White, D. R. Cayan, *J. Geophys. Res.* **103**, 21335 (1998).
9. R. C. Peterson, W. B. White, *J. Geophys. Res.* **103**, 24573 (1998).
10. M. Tsuchiya et al., *Prog. Oceanogr.* **23**, 101 (1989).
11. G. C. Johnson, M. J. McPhaden, *J. Phys. Oceanogr.* **29**, 3073 (1999).
12. R. D. Garreaud, D. S. Battisti, *J. Clim.* **12**, 2113 (1999).
13. N. E. Graham, *Clim. Dyn.* **10**, 135 (1994).
14. G. A. Jacobs et al., *Nature* **370**, 360 (1994).
15. K. E. Trenberth, J. W. Hurrell, *Clim. Dyn.* **9**, 303 (1994).
16. R. W. Reynolds, T. M. Smith, *J. Clim.* **7**, 929 (1994).
17. K. E. Trenberth, in *Teleconnections Linking Worldwide Climate Anomalies*, M. H. Glantz, R. W. Katz, N. Nicholls, Eds. (Cambridge Univ. Press, 1991), pp. 13–42.
18. We cut 7-mm-thick slabs of coral, which were cleaned in deionized water in an ultrasonic bath. Dry slabs were sampled with a low-speed microdrill along tracks parallel to corallite traces, as identified in x-ray positives, with a round diamond drill bit 1 mm in diameter.
19. We used an inductively coupled plasma atomic emission spectrophotometer at Harvard University to measure coral skeletal Sr/Ca, following a technique described in detail by D. P. Schrag [*Paleoceanography* **14**, 97 (1999)]. The external precision was better than 0.15% (relative standard deviation), based on analyses of replicate samples.
20. We measured oxygen isotopes on a gas source mass spectrometer with an individual acid reaction vessel system, following procedures outlined by B. K. Linsley, L. Ren, R. B. Dunbar, and S. S. Howe [*Paleoceanography* **15**, 322 (2000)]. External precision was better than 0.04‰ for  $\delta^{18}\text{O}$ , based on analyses of replicate samples.
21. To construct the chronology, we tied the annual minima in Sr/Ca and  $\delta^{18}\text{O}$  to February (on average the warmest month) and maximum Sr/Ca and  $\delta^{18}\text{O}$  to August/September (on average the coolest months). We also assumed that density bands in this coral skeleton are deposited annually.
22. B. K. Linsley, G. M. Wellington, D. P. Schrag, data not shown.
23. G. M. Wellington, R. B. Dunbar, G. Merlen, *Paleoceanography* **11**, 467 (1996).
24. Three-month running averages result in correlations to IGOSS SST of  $r^2 = 0.82$  for Sr/Ca and  $r^2 = 0.59$  for  $\delta^{18}\text{O}$ . We believe that the 3-month running average regression results may be more representative of the actual relation with SST, because the age model for the coral record may have uncertainties of 1 to 2 months.
25. J. W. Beck et al., *Science* **257**, 644 (1992).
26. S. de Villiers, G. T. Shen, B. K. Nelson, *Geochim. Cosmochim. Acta* **58**, 197 (1994).

27. C.-C. Shen et al., *Geochim. Cosmochim. Acta.* **60**, 3849 (1996).
28. C. Alibert, M. T. McMulloch, *Paleoceanography* **12**, 345 (1997).
29. Evaluation of the Comprehensive Ocean Atmosphere Data Set SST data for the 2°-by-2° region around Rarotonga reveals that near-continuous monthly data exist only back to 1960. The Global Ocean Surface Temperature Atlas data for the 5°-by-5° region around Rarotonga only contain near-continuous SST anomaly data back to 1950. Both SST databases contain virtually no measurements before 1930. Thus, we compared interannual and decadal changes in Sr/Ca to measured SST anomalies only back to 1950. The Climate Analysis Center (CAC) SST anomalies are from (16). The optimally smoothed (OS) SST anomaly data are from Kaplan et al. [*J. Geophys. Res.* **103**, 18567 (1998)]. Correlations between annually averaged coral Sr/Ca and annually averaged OS SST and CAC SST anomalies have  $r^2$  values of 0.45 and 0.37, respectively. Although these are lower than the correlation to 1°-by-1° IGOSS SST, they are both significant at the 99% level.
30. The Niño3/4 SST record reflects SST anomalies in the central equatorial Pacific region bounded by 5°S–5°N and 120°–170°W.
31. This observation is based on Singular Spectrum Analysis (SSA) of the Sr/Ca Series (1726–1997), using software written by E. Cook (Lamont-Doherty Earth Observatory). After bandpass filtering to remove the annual cycle and periods greater than 50 years, 37% of the variance is attributed to decadal and interdec-

adal variability and 43% of the variance to ENSO band (3- to 7-year) variability ( $n = 3244$  and window length = 120 months). In comparison, SST variability in the equatorial Niño3/4 region contains only 18% of variance in the decadal and interdecadal bands and 64% in the interannual band [based on the same SSA analysis of Kaplan OS SST anomaly data (29) for the Niño 3/4 region].

32. T. M. Quinn et al., *Paleoceanography* **13**, 412 (1998).
33. M. R. Rampino, S. Self, *Quat. Res.* **18**, 127 (1982).
34. R. B. Stothers, *Science* **224**, 1191 (1984).
35. H. H. Lamb, *Philos. Trans. R. Soc. London Ser. A* **266**, 425 (1970).
36. T. J. Crowley, T. M. Quinn, F. W. Taylor, C. Henin, P. Joannot, *Paleoceanography* **12**, 633 (1997).
37. J. E. Cole, R. B. Dunbar, T. R. McClanahan, N. Muthiga, *Science* **287**, 617 (2000).
38. Cross-spectral analysis was done on 2-year low-bandpass-filtered versions of Rarotonga Sr/Ca and the PDO with the ARAND software package, which is maintained and distributed by P. Howell of Brown University.
39. We thank O. Hoegh-Guldberg and J. Caselle for assistance with field sampling and E. Goddard and S. Howe for analytical assistance. Comments from two anonymous reviewers were also greatly appreciated. Supported by NSF grant ATM-9901649 and NOAA grant NA96GP0406 to B.K.L., NSF grant ATM-9619035 and NOAA grant NA96GP0470 to G.M.W., and NSF grants OCE-9733688 and OCE-9819257 to D.P.S.

8 June 2000; accepted 10 October 2000

## Contributions of Land-Use History to Carbon Accumulation in U.S. Forests

John P. Caspersen,<sup>1\*</sup> Stephen W. Pacala,<sup>1</sup> Jennifer C. Jenkins,<sup>2</sup> George C. Hurtt,<sup>3</sup> Paul R. Moorcroft,<sup>1</sup> Richard A. Birdsey<sup>4</sup>

Carbon accumulation in forests has been attributed to historical changes in land use and the enhancement of tree growth by CO<sub>2</sub> fertilization, N deposition, and climate change. The relative contribution of land use and growth enhancement is estimated by using inventory data from five states spanning a latitudinal gradient in the eastern United States. Land use is the dominant factor governing the rate of carbon accumulation in these states, with growth enhancement contributing far less than previously reported. The estimated fraction of aboveground net ecosystem production due to growth enhancement is  $2.0 \pm 4.4\%$ , with the remainder due to land use.

Although mid-latitude forests of the northern hemisphere are known to provide a large sink for atmospheric CO<sub>2</sub> (1–3), considerable uncertainty remains about the cause of the sink. Nitrogen deposition, CO<sub>2</sub> fertilization, and climate change have been shown to enhance tree

growth in forest ecosystems (4), but historical changes in land use also provide an alternative explanation for the sink, particularly the regrowth of forests after agricultural abandonment, reduced harvesting, and fire suppression (5). Assessing the relative contribution of land use and growth enhancement is critical for planning strategies to mitigate the accumulation of CO<sub>2</sub> in the atmosphere (6). If forests are simply regrowing in response to changes in land use, then the sink can be expected to saturate as forests regain their former biomass. However, if tree growth has been enhanced, then the future storage potential of forests is much less certain.

Estimates of the fraction of the forest sink due to regrowth versus enhancement vary widely, but growth enhancement has been consistently estimated to be large. In the United

<sup>1</sup>Department of Ecology and Evolutionary Biology, Princeton University, Princeton, NJ 08540, USA. <sup>2</sup>Northeastern Research Station, USDA Forest Service, Post Office Box 968, Burlington, VT 05402, USA. <sup>3</sup>Complex Systems Research Center, Institute for the Study of Earth, Oceans, and Space, University of New Hampshire, Durham, NH 03824, USA. <sup>4</sup>Northeastern Research Station, USDA Forest Service, 11 Campus Boulevard, Suite 200, Newtown Square, PA 19073, USA.

\*To whom correspondence should be addressed. E-mail: jpc@eno.princeton.edu

States, estimates of the fraction due to growth enhancement range from 25% (7) up to 75% (5), suggesting that the rate of biomass accumulation in U.S. forests has increased substantially over the last century. If this were the case, then growth enhancement should be readily observed by comparing current rates of accumulation with historical rates of accumulation (8).

Here, we examine whether growth enhancement has increased the rate of biomass accumulation in eastern U.S. forests using the Forest Inventory and Analysis (FIA) database (9–11). We restrict our analysis to five eastern states (Minnesota, Michigan, Virginia, North Carolina, and Florida), which provide the data necessary for estimating changes in biomass (12). For each of the more than 20,000 plots in the five-state sample, the data include estimates of aboveground biomass at the time of two successive inventories (the first in the late 1970s to mid-1980s and the second in the early to mid-1990s), changes in aboveground biomass due to growth and mortality (13), and the age of the plot in each of the two inventory periods (defined as the time since stand establishment after agricultural abandonment, clear-cutting, or stand-destroying natural disturbance) (14).

The best way to estimate historical changes in growth and mortality rates (hereafter referred to as vital rates) is with repeated measurements spanning the period of interest. However, this would require at least three inventories. How then can we estimate historical changes in vital rates with only a single measurement provided by the two inventories? The key is that in addition to stand age we also have a record of stand biomass, which is the cumulative result of past vital rates. The biomass  $B$  of a stand of age

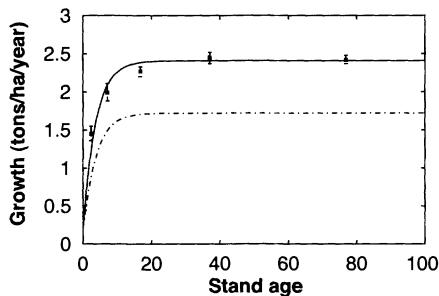


**Fig. 1.** The growth rate in the 1980s in Michigan (squares). Values are means  $\pm$  1 SE of the data, shown for five different age class bins. The small standard errors reflect the large sample size (2890 plots). The upper curve (solid line) is referred to as  $G(A)$ . If past growth rates were lower than the growth rate in the 1980s, then forest biomass would be lower than is observed. To illustrate, we present a hypothetical scenario in which we assume that growth before 1930 was given by the lower curve (dashed) and then increased linearly ( $\beta = 0.005$ ) until it reached the upper curve in 1980. The amount of biomass predicted to accumulate under the hypothetical scenario appears in Fig. 2.

$A$  is the sum of its gains from growth minus its losses from mortality over the previous  $A$  years. Therefore, if vital rates measured in the 1980s were unchanged from the past, we could predict the biomass of a stand of age  $A$  by calculating the difference between growth and mortality at each previous age, using the 1980s rates, and summing the difference over the previous  $A$  years. However, if growth rates were higher in the 1980s than in the past, or mortality rates were lower, then the biomass predicted using 1980s rates would be larger than observed. Thus, we can use the difference between the predicted and observed biomass to estimate past changes in the vital rates.

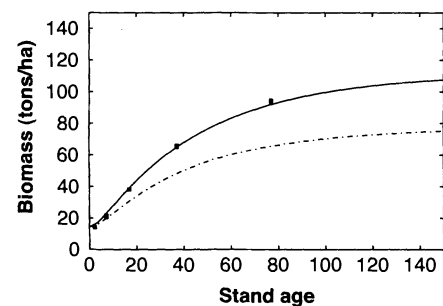
To illustrate this method, we present a deliberately simplified example using the Michigan inventory data for the 1980s. The first step is to estimate the current growth,  $G(A)$ , and the current mortality rate,  $\mu$  ( $\mu B = M$ , where  $M$  is the total amount of biomass lost to mortality) (15). Growth in Michigan increases rapidly with stand age as the canopy closes, and then remains approximately constant at about 2.4 tons/ha per year (Fig. 1). The mortality rate in Michigan (the fraction of biomass lost to mortality, including both natural mortality and selective harvesting) is 2.1% per year. Assuming that past vital rates were the same as the vital rates in the 1980s, we can calculate the expected relation between biomass and stand age,  $B(A)$ , using  $G(A)$  and  $\mu$ . For example, if  $B(0)$  is the initial biomass (the biomass present after clear-cutting, natural stand destruction, or agricultural abandonment), then the biomass of a 1-year-old stand is  $B(1) = B(0) + G(0) - \mu B(0)$ , the biomass of a 2-year-old stand is  $B(2) = B(1) + G(1) - \mu B(1)$ , and so on for any subsequent age. The biomass predicted from 1980's rates [ $B(A)_{pred}$ ] is given by the upper curve in Fig. 2 (16). Note that the vital rates measured in the 1980s accurately predict the observed biomass in the 1980s [ $B(A)_{pred} \approx B(A)_{obs}$ ], even though the observed biomass is the cumulative result of vital rates before the 1980s. The implication is that the vital rates in

the 1980s were not substantially different from historical vital rates, and therefore, there has been little or no growth enhancement.

To estimate the magnitude of growth enhancement, let  $G(A)f(t)$  be the growth rate of an age- $A$  stand  $t$  years ago, where  $f(t)$  specifies past changes in growth relative to the current growth rate,  $G(A)$ , and is equal to one at the time of the first inventory. Here, we assume for simplicity a linear function:  $f(t) = 1 - \beta t$ , although qualitatively similar results are obtained using other forms. Given  $G(A)f(t)$ , and the current mortality rate  $\mu$ , we can use the same iterative procedure described above for summing past vital rates to obtain a relation between biomass and stand age for different values of  $\beta$ . We estimate  $\beta$  as the value that provides the best fit to  $B(A)_{obs}$ . The estimated value of  $\beta$  is very small ( $\beta < 0.00001$ , indicating a growth enhancement of less than 0.001% per year), because  $B(A)_{pred} \approx B(A)_{obs}$ . In contrast, if past growth rates were significantly lower than the current growth rate, then forest biomass would be significantly lower than observed (see the hypothetical scenario presented in Figs. 1 and 2, in which growth enhancement is assumed to be large enough to cause 50% of current carbon accumulation).

Although the analysis presented above illustrates how, in principle, the magnitude of growth enhancement can be estimated from inventory data, two issues must be addressed to make the analysis rigorous. First, we must account for the strong correlations that develop between growth, mortality, and biomass because of spatial and temporal variation in growth and mortality. Second, we must allow for the possibility that a difference between predicted and observed biomass could be due to changes in mortality, as well as changes in growth. To address these issues, we derive a maximum likelihood estimator (17), based on the joint probability of  $B(A)$ ,  $G$ , and  $M$ , to account for correlated errors in these variables. We also include a function  $h(t)$  that specifies past changes in mortality rates in the same way

**Fig. 2.** Observed biomass [ $B(A)_{obs}$ ] in Michigan in 1980 (squares). Values are means  $\pm$  1 SE.  $B(A)_{pred}$  (solid line), the amount of biomass predicted to accumulate at current growth and mortality rates, assumes no growth enhancement. Note that the current mortality rate includes both natural mortality and selective harvesting, so the asymptotic biomass is lower than would be expected in undisturbed old-growth forests. The amount of biomass predicted to accumulate under the hypothetical scenario (dashed line) assumes that growth before 1930 was given by the lower curve in Fig. 1 and then increased linearly ( $\beta = 0.005$ ) until it reached the upper curve in Fig. 1 in 1980. The hypothetical accumulated biomass lies many standard errors below the observed biomass, because the hypothesis that growth was lower in the past is not consistent with the observed biomass. We chose this scenario because, if it were true, then 50% of total forest biomass accumulation in Michigan during the 1980s would have been due to growth enhancement. The implication is that the method provides the sensitivity necessary to assess the magnitude of growth enhancement.



that  $f(t)$  specifies past growth rates:  $h(t) = 1 + \alpha t$ , where positive values of  $\alpha$  indicate a decrease in mortality from past to present (18). Although a decrease in mortality would cause  $B(A)_{\text{pred}}$  to exceed  $B(A)_{\text{obs}}$ , as would an increase in growth, the estimator can separate changes in growth and mortality, because each has a distinct effect on the relation between biomass and stand age (19).

The maximum likelihood estimates show that in each of the five states, the value of  $\beta$  is less than 0.0001, indicating that the annual average increase in growth is less than 0.01% (Table 1). In Minnesota, Michigan, and Florida, the estimated annual change in the rate of mortality is also small, because  $B(A)_{\text{pred}} \approx B(A)_{\text{obs}}$ . In contrast, we estimate an annual average decrease in mortality of 4.9% and 2.8% in Virginia and North Carolina, because  $B(A)_{\text{pred}} > B(A)_{\text{obs}}$ , but primarily in older stands (20). The estimated decrease in mortality likely reflects a decrease in the rate of selective harvesting.

From our estimates of  $\beta$ , we calculate the fraction of biomass accumulation due to growth enhancement using two different measures of aboveground net ecosystem production (ANEP). The first is the stand-level ANEP which is the net accumulation of biomass [ $B(A + 1) - B(A)$ ] in stands that were not clear-cut or otherwise heavily disturbed (15). For these stands we calculate ANEP

with the estimated growth enhancement ( $ANEP_{\text{with}}$ ) and also with the enhancement stopped  $t$  years before the first census ( $ANEP_{\text{without}}$ ): the fraction due to growth enhancement equals  $1.0 - ANEP_{\text{without}}/ANEP_{\text{with}}$ . For example, if growth had not increased after 1930, the average stand-level ANEP for all five states would be 1.588 tons/ha per year instead of 1.597 tons/ha per year. Thus, Fig. 3 shows that 0.44% of stand-level ANEP (solid squares) is due to changes in growth that have occurred since 1930 (21). At a broader scale, much of the biomass accumulation is offset by losses caused by large-scale disturbances such as clear-cutting and the conversion of forested land to non-forested land. Thus, we calculate a regional-level ANEP, with and without growth enhancement, for each state by including losses due to large-scale disturbance, as well as gains due to reforestation (22). The upper confidence bounds of the estimates indicate the fraction of regional ANEP due to growth enhancement is no greater than 7.0% (23).

Because the results demonstrate that carbon accumulation is overwhelmingly due to forest regrowth rather than growth enhancement, we conclude that land-use change is the dominant factor governing the rate of carbon accumulation in eastern U.S. forests. It is possible that growth enhancement by N deposition and CO<sub>2</sub>

fertilization is balanced by the negative effects of other factors such as ozone and calcium depletion. However, such balancing effects on growth cannot be readily evaluated with the FIA data. Our results have several implications for the effort to predict and model the fate of the terrestrial carbon sink. First, since regrowth accounts for the vast bulk of the carbon accumulating in the forests we studied, carbon accumulation in forests may be expected to attenuate at a predictable rate as forests recover their former biomass. Second, ecosystem models that focus exclusively on physiological processes omit the dominant factor governing the rate of carbon sequestration in forests, namely, land-use history. Finally, ecosystem models that account for land-use history, stand age, and stand structure may be expected to predict gross carbon fluxes in forests despite considerable uncertainty regarding the effects of N deposition, CO<sub>2</sub> fertilization, and climate change.

References and Notes

- R. K. Dixon et al., *Science* **263**, 185 (1994).
- R. A. Birdsey, L. S. Heath, in *Productivity of America's Forests and Climatic Change, General Technical Report RM-GTR-271*, L. A. Joyce, Ed. (U.S. Department of Agriculture (USDA), Forest Service, Rocky Mountain Forest and Range Experiment Station, Fort Collins, CO, 1995), pp. 56–70.
- H. Spiecker, K. Mielikainen, M. Kohl, J. P. Skovsgaard, Eds. *Growth Trends in European Forests* (Springer-Verlag, Berlin, 1996).
- H. A. Mooney et al., in *The Terrestrial Biosphere and Global Change: Implications for Natural and Managed Ecosystems*, B. H. Walker, W. L. Steffen, J. Canadell, J. S. I. Ingram, Eds. (Cambridge Univ. Press, Cambridge 1999), pp. 141–189.
- R. A. Houghton, J. L. Hackler, K. T. Lawrence, *Science* **285**, 574 (1999).
- International Geosphere-Biosphere Programme (IGBP) Terrestrial Carbon Working Group, *Science* **280**, 1393 (1998).
- D. Schimel et al., *Science* **287**, 2004 (2000);
- Numerous studies of the historical changes in timber yields in Europe indicate that yield has increased in some regions (3). However, because improved silvicultural practices in these highly managed forests are known to have increased yield, the increased growth is not necessarily the result of N deposition, CO<sub>2</sub> fertilization, or climate change.
- The FIA database is publicly available at: [www.srsfia.usfs.msstate.edu/scripts/ew.htm](http://www.srsfia.usfs.msstate.edu/scripts/ew.htm).
- M. H. Hansen, T. Frieswyk, J. F. Glover, J. F. Kelly, *USDA Forest Service Gen. Tech. Rep. NC-151* (1992).
- R. A. Birdsey, H. T. Schreuder, *USDA Forest Service Gen. Tech. Rep. RM-214* (1992).
- Supplementary material is available to *Science* Online subscribers at [www.sciencemag.org/feature/data/1053700.shl](http://www.sciencemag.org/feature/data/1053700.shl).
- See (12).
- The age of a stand is determined from historical inventory records or estimated by measuring the age of representative site trees using growth rings. In most cases, the age of a stand is recorded to the nearest year. In some cases, however, stand age is recorded in 10-year age classes and the value recorded is the center of the age class (10).
- To quantify current vital rates, we selected plots that may have been selectively harvested but were not clear-cut or otherwise heavily disturbed after the first inventory. We excluded clear-cut or heavily disturbed plots by eliminating plots whose age was reset in the second inventory. In addition, we excluded plots occurring in plantations and plots that were classified as nonforest in either the first or the second inventory. We specify growth with an asymptotic Michaelis-Menten function:  $G(A) = c + d[1 - \exp[-(k/d)A]] + \epsilon$ , where

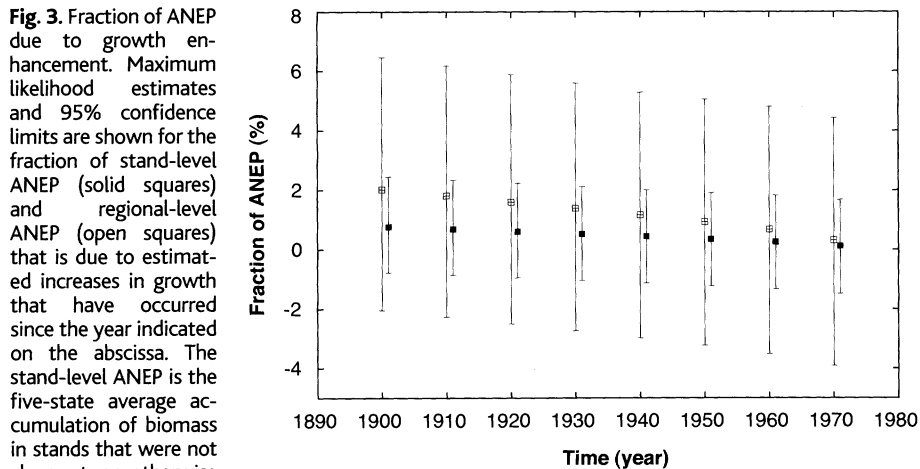


**Fig. 3.** Fraction of ANEP due to growth enhancement. Maximum likelihood estimates and 95% confidence limits are shown for the fraction of stand-level ANEP (solid squares) and regional-level ANEP (open squares) that is due to estimated increases in growth that have occurred since the year indicated on the abscissa. The stand-level ANEP is the five-state average accumulation of biomass in stands that were not clear-cut or otherwise heavily disturbed. The region-level ANEP is the five-state average accumulation of biomass for all forested lands including losses due to large-scale disturbance such as clear-cutting.

**Table 1.** Maximum likelihood estimates and 95% confidence limits for  $\alpha$  and  $\beta$ . Positive values of  $\alpha$  indicate a decrease in mortality from past to present. Positive values of  $\beta$  indicate an increase in growth from past to present. A value of 0.0001 indicates a 0.01% annual change relative to the current rate. FL, Florida; MI, Michigan; MN, Minnesota; NC, North Carolina; and VA, Virginia.

	MN	MI	VA	NC	FL	
$\alpha$	Upper	0.0000025	0.0019909	0.0482061	0.0311884	0.0012190
	Lower	-0.0000071	0.0018596	0.0478810	0.0296815	0.0006871
$\beta$	Upper	-0.0000675	0.0017049	0.0464871	0.0267182	0.0000002
	Lower	0.0001039	0.0000921	0.0001069	0.0000507	0.0001692
$\beta$	Upper	0.0000610	0.0000368	0.0000953	0.0000493	0.0000656
	Lower	0.0000405	0.0000109	0.0000755	0.0000306	0.0000095

$\varepsilon \sim N(0, i + jG)$ . Although growth exhibits a slight decline with stand age in some cases, using alternative functional forms that allow for a decline do not significantly change the results presented here. We specify mortality as an exponential random variable with mean  $M = \mu B$ , where the mortality rate  $\mu$  is a constant. Although the mortality rate exhibits a slight decline with stand age in some cases, using alternative functional forms that allow for a decline do not significantly change the results presented here (the stand mortality rate reflects mortality from various sources, including thinning, windthrow, fire, and selective harvesting, which may exhibit different trends with respect to stand age). We obtained maximum likelihood estimates of the growth and mortality parameters using a simulated annealing algorithm as we do in all subsequent analyses.

16. Given  $G(A)$  and  $\mu$ , we can calculate  $B(A)$  for any value of  $B(0)$ . We estimate  $B(0)$  as the value that provides the best fit to  $B(A)_{\text{obs}}$ . Here, we assume that  $B(A)_{\text{obs}}$  is normally distributed with constant variance.
17. See (12).
18. In this paper we report results for linear forms of  $h(t)$  and  $f(t)$ , although alternative forms give similar results.
19. Changes in mortality disproportionately affect old high-biomass stands, because the amount of biomass lost to mortality is small relative to growth in young low-biomass stands but not in old high-biomass stands. Thus, if mortality rates have decreased, current vital rates will closely predict the biomass of younger stands but the predicted biomass of older stands will exceed the observed biomass. In this case, a nonzero  $\alpha$  will provide a better fit to  $B(A)_{\text{obs}}$  than a nonzero  $\beta$ . On the other hand, if growth rates have increased, the predicted biomass will exceed the observed biomass in both young and old stands. In this case, a nonzero  $\beta$  will provide a better fit to  $B(A)_{\text{obs}}$  than a nonzero  $\alpha$ .
20. The estimates in Table 1 indicate that the rate of biomass accumulation has not increased in MN, MI, and FL. In VA and NC, there has been an increase in the rate of biomass accumulation, but we estimate that this increase is due to decreases in mortality rather than increases in growth. The disproportionate effect of changes in growth and mortality on old versus young stands allows us to partition increased accumulation between increases in growth and decreases in mortality. Yet, one can always conceive of complicated scenarios in which changes in mortality exactly balance changes in growth in both old stands and young stands, making partitioning impossible. For this reason, we also present independent evidence that confirms our conclusion that there has been a reduction in mortality in Virginia and North Carolina rather than an increase in growth. See (12).
21. These estimates are based on allometric equations used to estimate the aboveground biomass of trees. Thus, if N deposition, CO<sub>2</sub> fertilization, or climate change had a pronounced effect on tree allometry (by significantly increasing the ratio of root biomass to total tree biomass), then the fraction of total net ecosystem production (above and below ground) due to growth enhancement could be greater than the fraction of ANEP due to growth enhancement. Furthermore, growth enhancement may represent a small fraction of ANEP, because the effects of N deposition and CO<sub>2</sub> fertilization are balanced by the effects of other factors such as ozone and calcium depletion.
22. We calculate regional-level ANEP as the sum of the ANEP of natural stands that have not been clear-cut or otherwise heavily disturbed, and the ANEP of all the remaining plots, including clear-cut plots, plantations, and plots that changed from forest to nonforest and vice versa. For the remaining plots, we assumed zero biomass for plots classified as nonforest.
23. We obtain 95% confidence limits by calculating the fraction of ANEP due to growth enhancement using the range of parameter values for which the log-likelihood of the data is within 1.92 of the maximum log-likelihood (17). The highest and lowest fraction are the reported limits for the fraction of ANEP due to growth enhancement.

24. This research was conducted under the auspices of the Carbon Modeling Consortium (CMC), which is supported by the Office of Global Programs and the Geophysical Fluid Dynamics Laboratory of the NOAA. Support was also provided by the Andrew W. Mellon foundation. The advice and

insights provided by our colleagues at the CMC and elsewhere are gratefully acknowledged, in particular E. Shevliakova, J. Sarmiento, and M. Gloor.

5 July 2000; accepted 29 September 2000

## The Evolutionary Fate and Consequences of Duplicate Genes

Michael Lynch<sup>1\*</sup> and John S. Conery<sup>2</sup>

Gene duplication has generally been viewed as a necessary source of material for the origin of evolutionary novelties, but it is unclear how often gene duplicates arise and how frequently they evolve new functions. Observations from the genomic databases for several eukaryotic species suggest that duplicate genes arise at a very high rate, on average 0.01 per gene per million years. Most duplicated genes experience a brief period of relaxed selection early in their history, with a moderate fraction of them evolving in an effectively neutral manner during this period. However, the vast majority of gene duplicates are silenced within a few million years, with the few survivors subsequently experiencing strong purifying selection. Although duplicate genes may only rarely evolve new functions, the stochastic silencing of such genes may play a significant role in the passive origin of new species.

Duplications of individual genes, chromosomal segments, or entire genomes have long been thought to be a primary source of material for the origin of evolutionary novelties, including new gene functions and expression patterns (1–3). However, it is unclear how duplicate genes successfully navigate an evolutionary trajectory from an initial state of complete redundancy, wherein one copy is likely to be expendable, to a stable situation in which both copies are maintained by natural selection. Nor is it clear how often these events occur.

Theory suggests three alternative outcomes in the evolution of duplicate genes: (i) one copy may simply become silenced by degenerative mutations (nonfunctionalization); (ii) one copy may acquire a novel, beneficial function and become preserved by natural selection, with the other copy retaining the original function (neofunctionalization); or (iii) both copies may become partially compromised by mutation accumulation to the point at which their total capacity is reduced to the level of the single-copy ancestral gene (subfunctionalization) (1–12). Because the vast majority of mutations affecting fitness are deleterious (13), and because gene duplicates are generally assumed to be functionally redundant at the time of origin,

virtually all models predict that the usual fate of a duplicate-gene pair is the nonfunctionalization of one copy. The expected time that elapses before a gene is silenced is thought to be relatively short, on the order of the reciprocal of the null mutation rate per locus (a few million years or less), except in populations with enormous effective sizes (11, 12).

These theoretical expectations are only partially consistent with the limited data that we have on gene duplication. First, comparative studies of nucleotide sequences suggest that although both copies of a gene may often accumulate degenerative mutations at an accelerated rate following a duplication event, selection may not be relaxed completely (14–16). Second, the frequency of duplicate-gene preservation following ancient polyploidization events, often suggested to be in the neighborhood of 30 to 50% over periods of tens to hundreds of millions of years (17–20), is unexpectedly high.

Further insight into the rates of origin of duplicate genes and their evolutionary fates can now be acquired by using the genomic databases that have emerged for several species. We focused on nine taxa for which large numbers of protein-coding sequences are available through electronic databases: human (*Homo sapiens*), mouse (*Mus musculus*), chicken (*Gallus gallus*), nematode (*Caenorhabditis elegans*), fly (*Drosophila melanogaster*), the plants *Arabidopsis thaliana* and *Oryza sativa* (rice), and the yeast *Saccharomyces cerevisiae*. For each of these species, the complete set of available open reading frames was screened to eliminate se-

<sup>1</sup>Department of Biology, University of Oregon, Eugene, OR 97403, USA. <sup>2</sup>Department of Computer and Information Science, University of Oregon, Eugene, OR 97403, USA.

\*To whom correspondence should be addressed. E-mail: mlynch@oregon.uoregon.edu